https://doi.org/10.2352/EI.2026.38.7.IMAGE-274
©2026 Society for Imaging Science and Technology

Topological Adaptive Weighted Drug-target Affinity Prediction

Linman Du [a], Wenzong Jiang [b], Bin Shen [c], Weifeng Liu [a], Baodi Liu [a,]*
[a] College of Control Science and Engineering, China University of Petroleum (East China), Qingdao, China
[b] College of Oceanography and Space Informatics, China University of Petroleum (East China), Qingdao, China
[c] Celonis, New York, United States
** Corresponding author*

Abstract

Accurate prediction of drug target affinity (DTA) is critical for accelerating drug discovery, yet existing methods often struggle with topological diversity and insufficient feature extraction in molecular graphs. This paper proposes a novel framework, Topological Adaptive Weighted Drug Target Affinity Prediction (TAW-DTA), which integrates a Topological Adaptive Graph Convolutional Network (TAGCN) and a gated skip-connection mechanism to address these limitations. TAGCN dynamically adjusts convolution filters based on node topology, enabling robust feature extraction from drug molecular graphs and weighted protein contact maps. The gated skip-connection mechanism mitigates gradient vanishing and feature degradation in deep networks by selectively fusing multiscale features. Evaluations of benchmark data sets demonstrate state-of-the-art performance, with improvements in the concordance index (CI) and reduced prediction errors. Ablation studies confirm the efficacy of TAGCN and the skip-connection mechanism. This framework offers a scalable and interpretable solution for DTA prediction, with significant potential for practical drug development applications.

Introduction

The core goal of drug discovery is to identify compounds that can bind to specific targets and influence disease progression. Traditional methods, such as protein microarrays and affinity chromatography, are time-consuming and costly. Therefore, computer-based drug target affinity (DTA) prediction methods have gained attention due to their efficiency and low cost [1, 2].

Before deep learning, DTA prediction relied on molecular docking and molecular dynamics simulations, which required precise three-dimensional (3D) structural information of molecules and proteins. However, these methods were inefficient when 3D structures were unavailable. Traditional machine learning methods, such as linear regression and random forest regression, could predict DTA based on textual descriptions, reducing the need for 3D structural information. These methods used the Simplified Molecular Input Linear Expression (SMILES) to encode small molecule drugs and assessed drug-protein interactions using metrics like the dissociation constant (K_d), inhibition constant (K_i), or IC_{50}.

Deep learning has improved DTA prediction by automatically extracting high-level latent features derived from drug and target sequences as well as structures. Current deep learning-based DTA prediction methods are divided into sequence-based and structure-based approaches. Sequence-based methods use text embeddings and convolutional neural networks (CNNs), but they neglect structural features. Structure-based methods, such as GraphDTA, use graph neural networks (GNNs) to represent drug molecules. However, they often overlook the structural information in protein sequences.

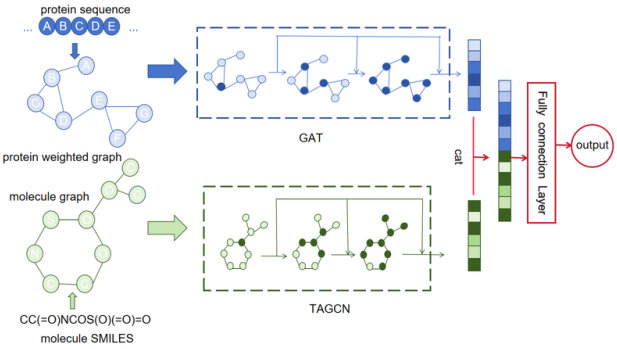

Figure 1. *The overall architecture of TAW-DTA. It includes a data preprocessing module, a drug feature extraction module, a protein feature extraction module, a feature fusion module and a regression prediction module.*

To address these limitations, we developed a novel topological adaptive weighted graph neural network (GNN) prediction framework. This framework introduces TAGCN, which adapts to the topological diversity of nodes by counting the number of neighbors of each node. It also incorporates a gated skip connection mechanism to solve the problem of gradient vanishing and node feature degradation in deep GNNs. Our model constructs drug atom maps and weighted protein maps to learn representations from multiple perspectives. Experimental results show that our model outperforms existing methods, with lower prediction errors and higher stability.

In summary, our contributions include:

1. Constructing drug atom maps and weighted protein maps to fully utilize topological information.

2. Introducing TAGCN, which adapts to the topology of different nodes.

3. Implementing a gated hopping connection mechanism to retain topological features at different scales.

Materials and Methods

We developed a novel dual-channel prediction framework for drug-target interaction strength. It uses contact maps to model protein 3D conformations and topological graphs for molecular characterization. By integrating TAGCN, GAT, and gated skipping strategies, it enhances feature extraction and prediction accuracy, as shown in experiments (Fig. 1).

Weighted Protein Maps and Potential Vector Extraction

This study developed an innovative protein contact map prediction framework. It uses the ESM model to construct weighted protein maps, significantly boosting structure prediction efficiency. Proteins' one-dimensional amino acid sequences (typically 20-25 amino acids) fail to fully characterize their 3D spatial conformations, while their biological functions mainly rely on spatial structural features like hydrogen bonds and ionic interactions. Despite the expanding protein databases, much protein structure information remains unresolved. Thanks to advances in natural language processing, new-generation protein language models [4, 5, 6] enable direct sequence-to-structure prediction.

We implemented Rao et al.'s ESM method to predict protein contact maps in under 60 seconds. Residue interaction intensity was quantified via a probability matrix (range [0,1]), establishing a protein network with weighted properties, with residues functioning as nodes, interactions operating as edges, and continuous probability values acting as edge weights. To enhance efficiency, we removed the computationally intensive PSSM and screened key residue features.

To address the ESM model's sequence length constraint ($\leq$ 1024 residues), we adopted a segmented prediction strategy. Long sequences ($>$ 1000 residues) were divided into segments based on length L and step $L/2$, with the complete contact map obtained by averaging overlapping regions. We also constructed 33-dimensional feature vectors for each residue, incorporating attributes including attributes like type, polarity, hydrophobicity, molecular weight, and group dissociation constants—these act as high-caliber inputs for deep learning analyses.

We used a weighted GNN (specifically GAT) to extract protein features and establish TAW-DTA. GAT's attention mechanism adaptively learns node weights, capturing interaction intensity more accurately than GCN's fixed aggregation, handling both strong (e.g., hydrogen bonds) and weak (e.g., hydrophobic) interactions, and efficiently processing sparse maps to identify key residue pairs.

GAT learns node hidden representations via self-attention: nodes are linearly transformed by $W \in R^{F^0}$; attention coefficients between node i and neighbor j are calculated via Equations 1-2; Softmax normalizes weights (sum=1, indicating node pair importance); LeakyReLU enhances model stability/robustness (superior to ReLU for negative inputs); Equation 3 aggregates adjacent node features by attention scores to get hidden layer representations.

$$e_{ij} = a\left(WX_i \| WX_j\right) \tag{1}$$

$$\alpha_{ij} = \text{softmax}\left(e_{ij}\right) = \frac{\exp\left(\text{LeakyReLU}\left(e_{ij}\right)\right)}{\sum_{k\in N_i}\exp\left(\text{LeakyReLU}\left(e_{ik}\right)\right)} \tag{2}$$

$$h_i = \sigma\left(\sum_{j\in N_i}\alpha_{ij}WX_j\right) \tag{3}$$

where $X_i \in R^d$ denotes the input feature vector of node i, $\mathcal{N}_i$ represents its neighborhood node set, e_{ij} indicates the raw attention score between nodes (i, j), $\alpha_{ij} = \text{softmax}(e_{ij})$ is the normalized attention coefficient via nonlinear activation, $h_i^{(l)}$ corresponds to the hidden representation at layer l, $\sigma(\cdot)$ denotes the nonlinear activation function (e.g., ReLU), with $\mathbf{W} \in R^{d'\times d}$ being the trainable parameter matrix and $\mathbf{a}$ the shared attention mechanism weights.

In TAW-DTA, our architecture employs three stacked graph neural network (GNN) layers to learn node embeddings $\mathbf{Z} \in R^{N\times F}$, where N denotes the maximum node count and F represents the feature dimension. To address variable-sized molecular graphs (with differing atom counts for compounds and residue numbers for proteins), we apply global mean pooling once the final GNN layer is completed, features specific to each node are aggregated into graph-level representations of fixed dimension $\mathbf{g} \in R^F$. Subsequent processing through three fully-connected layers with ReLU activation and dropout (rate=0.3) progressively reduces dimensionality, ultimately yielding a 128-dimensional interaction descriptor $\mathbf{d} \in R^{128}$ for binding affinity prediction.

Construction of Molecular Diagrams and Extraction of Latent Vectors

To enhance the representation of chemical and topological information for drug molecules, we utilized RDKit [7] to convert the SMILES sequence of the drug into a molecular graph. This approach allows for a more comprehensive characterization of drug molecules by representing them as graphs, where nodes correspond to atoms and edges represent chemical bonds. In this molecular graph representation, each node (atom) is associated with several key features: the atomic symbol, the number of adjacent atoms, the number of adjacent hydrogen atoms, the valence of the atom, and whether the atom is part of an aromatic ring structure [8].

The 2D undirected molecular graph of the drug can be formally defined as $G^D = (V^D, E^D)$, where V^D is the set of atomic nodes and E^D is the set of edges representing chemical bonds. Each node $V_i^D \in V^D$ is characterized by its atomic features, while each edge $E_{ij}^D \in E^D$ indicates the presence of a chemical bond between nodes i and j. The adjacency matrix $A^D \in R^{N\times N}$ is used to represent the connectivity of the graph, where $A_{ij}^D = 1$ if there is an edge between the nodes i and j, and $A_{ij}^D = 0$ otherwise, indicating that there is no chemical bond between the two nodes.

Figure 2 illustrates the node and edge features employed in our method to construct drug maps, which have been previously utilized in studies to represent drug molecules. This structured representation enables a detailed analysis of both chemical and topological properties, providing a foundation for further computational analysis and modeling. In the TAW-DTA algorithm, GNNs are used to extract features from graph-structured data. As a novel deep learning architecture, GNNs surpass the constraints of CNNs, which are limited to processing fixed-dimensional Euclidean data. In contrast, GNNs excel at handling non-Euclidean data, making them suitable for complex graph structures. Among various variants of GNN, GCNs are widely utilized. However, GCNs have notable limitations: their single-scale convolutional design restricts multiscale feature extraction; uniform convolutions fail to accommodate varying node topologies; and deeper networks often lead to feature oversmoothing, causing critical structural information loss.

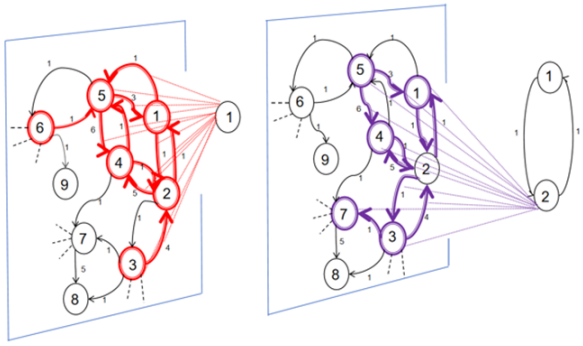

Figure 2. *An example of a directed graph with edge weights defined by matrix A. The left (right) portion, highlighted with a halo, illustrates the filter positioned at different vertices. The left graph depicts filtering/convolution initiated at vertex 1. As the filter shifts to vertex 2 (right graph), its topology dynamically adapts to the new local neighborhood.*

To address these issues, the TAGCN offers a superior alternative for feature extraction in drug molecular graphs. TAGCN employs multi-scale convolutional kernels to capture both local and global structural details, overcoming GCN's single-scale limitation. Moreover, its topology-adaptive convolution dynamically adjusts weights based on node-specific topologies, effectively modeling complex chemical interactions. This adaptability enables TAGCN to precisely extract features like functional groups and ring structures in molecular graphs.

TAGCN further mitigates the feature over-smoothing issue through a hierarchical aggregation mechanism. By selectively retaining key node features, it prevents homogenization in deep networks, ensuring distinct molecular characteristics are preserved. This is crucial for accurately predicting drug-target interactions, where subtle molecular differences significantly impact binding affinity.

TAGCN represents a drug molecule as a graph $G = (V, E)$, with nodes V (atoms) and edges E (bonds). Each node v_i has a feature vector h_i. TAGCN updates these features using K convolutional kernels. For each kernel k, node v_i's feature is updated via:

$$h_i^{(k)} = \sum_{v_j \in \mathcal{N}(v_i)} \frac{1}{\sqrt{|\mathcal{N}(v_i)| \cdot |\mathcal{N}(v_j)|}} W^{(k)} h_j \tag{4}$$

Here, $\mathcal{N}(v_i)$ is the neighbor set of v_i, and $W^{(k)}$ is the kernel's weight matrix.

To accommodate topological variations, TAGCN computes adaptive weights α_{ij} using:

$$\alpha_{ij} = \text{softmax}\left(\text{MLP}\left(h_i \| h_j\right)\right) \tag{5}$$

where MLP is a multi-layer perceptron, and $\|$ denotes concatenation.

Finally, the updated feature h_i' is obtained by:

$$h_i' = \sigma\left(\sum_{k=1}^{K} \sum_{v_j \in \mathcal{N}(v_i)} \alpha_{ij} h_i^{(k)}\right) \tag{6}$$

Here, σ is a non-linear activation function.

Gated Skip-Connection Mechanism

To capture long-range neighborhood information in a specific central atom, multiple GNN layers are typically stacked. However, with an increase in the number of GNN layers, issues such as gradient vanishing and node feature degradation may arise. To address these challenges, aZS gated skip-connection mechanism is introduced into the representation learning of every hidden layer. By adjusting the rates of forgetting and updating, this mechanism fuses features from different hidden states, enabling each node to aggregate information from remote nodes while preserving its unique characteristics as the model depth increases.

The gated skip-connection mechanism is formulated as shown in Equations 7 and 8. Here, U_1 and U_2 are trainable parameters, b is the bias term, $H_i^{(l)}$ and $H_i^{(l+1)}$ represent the feature vectors of node i at the l-th and $(l+1)$-th layers, respectively, and z_i represents the learned proportion coefficient used to retain information from the preceding hidden layer. We select a sigmoid activation function to guarantee that the learned proportion coefficient remains in the range of 0 to 1.

$$z_i = \text{sigmoid}\left(U_1 H_i^{(l+1)} + U_2 H_i^{(l)} + b\right) \tag{7}$$

$$H_i^{(l+1)} = z_i H_i^{(l+1)} + (1 - z_i) H_i^{(l)} \tag{8}$$

Experiments and Results

Datasets

This study utilized two publicly accessible datasets for experimentation. The Davis dataset [9] investigated interactions between 72 kinase inhibitors and 442 kinases, using the logarithmic transformation of dissociation constants (ρK_d) as the output metric for binding affinity.

The KIBA dataset [10], on the other hand, encompasses binding affinity measurements for 2,116 kinase inhibitors and 229 kinases. These values reflect the biological activities of kinase inhibitors as determined by the KIBA method, which integrates multiple indicators of inhibitor potency, including K_i, K_d, and IC_{50}.

Evaluate Metrics

To evaluate the model's performance on a specific dataset, we employed three metrics: the CI) [11], MSE and Root Mean Squared Regression (r_m^2), comparing these results with those of the baseline model.

CI is a critical metric for assessing the accuracy of predictive models, quantifying the alignment between predicted outcomes and observed results. It is calculated as follows:

$$CI = \frac{1}{Z} \sum_{\delta_j > \delta_i} h(b_i - b_j) \tag{9}$$

where b_i and b_j represent the predicted values of δ_i and δ_j, respectively, Z is a normalization hyperparameter, and $h(x)$ is a step function defined as:

$$h(x) = \begin{cases} 0, & x < 0 \\ 0.5, & x = 0 \\ 1, & x > 0 \end{cases} \tag{10}$$

MSE is a standard loss function for regression tasks, measuring the average squared difference between predicted and actual values. Its formula is:

$$MSE = \frac{1}{n}\sum_{i=1}^{n}(y_i - \tilde{y}_i)^2 \tag{11}$$

For the evaluation of TAW-DTA, we utilized a modified version of MSE to assess the model's generalization capability. This metric evaluates the discrepancy between predicted and true values and performs regression analysis to quantify the model's performance. Specifically, for the i-th sample, $\tilde{y}_i$ denotes the predicted value, while y_i represents the true value.

r_m^2 serves as an indicator of the model's generalization ability. A value exceeding 0.5 suggests acceptable generalization performance, while higher values indicate superior generalization capabilities. Mathematically, r_m^2 is defined as:

$$r_m^2 = r^2\left(1 - \sqrt{r^2 - r_0^2}\right) \tag{12}$$

where r is the squared correlation coefficient with intercept, and r_0 is the coefficient without intercept.

Performance on the Benchmark Dataset

To evaluate the performance of our model in predicting compound-target binding affinity, we compared it with ten baseline models: KronRLS, SimBoost, MT-DTI, MATT-DTI, GraphDTA, MRBDTA, DeepGLSTM, MGraph-DTA, WGNN-DTA, and DGraph-DTA. In order to ensure fairness in comparison, we used the same dataset partitioning strategy as GraphDTA, splitting the Davis and KIBA datasets into training and test subsets. The model was trained on the training set using the hyperparameters mentioned above, and the trained model was then used to predict the binding affinity of compounds and targets in the test set.

In Table 1, we present a comparative analysis of the performance of various models on the Davis dataset, including TAW-DTA, and their results on the KIBA dataset. The results demonstrate that TFUM-DTA outperforms the baseline model across all three evaluation metrics on the Davis dataset, with a significant improvement of 0.003 in *CI* compared to the previous state-of-the-art DGraph-DTA model. Additionally, on the KIBA dataset, TAW-DTA shows the best performance, compared to the previous best model, the CI improved by 0.001. For methods with multiple architectures, we similarly compared our model only with the best results on the Davis dataset to ensure fairness in evaluation.

Table 1: Performance on the Benchmark Dataset

Dataset	Model	CI	MSE
Davis	KronRLS [12]	0.871	0.379
	SimBoost [13]	0.872	0.282
	MT-DTI [14]	0.887	0.245
	MATT-DTI [15]	0.891	0.227
	GraphDTA [16]	0.893	0.229
	Attention-DTA [17]	0.888	0.195
	AttentionMGT-DTA [21]	0.891	0.193
	MGraph-DTA [19]	0.900	0.207
	WGNN-DTA [3]	0.903	0.208
	DGraph-DTA [20]	0.904	0.202
	TAW-DTA	**0.908**	0.202
KIBA	KronRLS [12]	0.782	0.441
	SimBoost[13]	0.836	0.222
	MT-DTI [14]	0.882	0.152
	MATT-DTI [15]	0.889	0.150
	GraphDTA [16]	0.891	0.139
	Attention-DTA [17]	0.880	0.158
	AttentionMGT-DTA [21]	0.893	0.140
	MGraph-DTA [19]	0.902	0.128
	WGNN-DTA [3]	0.898	0.130
	DGraph-DTA [20]	0.904	0.126
	TAW-DTA	**0.905**	**0.125**

Ablation Experiments

We conducted ablation studies to evaluate the contributions of the TAGCN and the gated skip connection mechanism. The experimental settings are as follows:

1) **Without TAGCN**: The model uses a traditional GCN for feature extraction of drug molecular graphs.

2) **Without gated skip connections**: The model replaces the skip connection mechanism with direct convolutional modules for learning target sequence representations.

Table 2 compares the performance of our full model and its two variants on the Davis dataset. Overall, our proposed model outperformed all three variants, confirming the following:

1) TAGCN better captures the structural features of molecular graphs compared to traditional GCN.

2) By selectively preserving topological features at different scales, the gated skip connection mechanism improves the model's performance.

The results highlight the importance of both components in improving the model's ability to predict compound-target interactions.

Table 2: The individual contributions of UniMP,ECA-Net and TFAM are verified on the Davis dataset

Davis	Without TAGCN	Without gated skip connections	TAW-DTA
MSE	0.206	0.211	0.202
CI	0.906	0.897	0.907

Model Evaluation of Compound-Protein Interaction Tasks

This article evaluates the TAW-DTA model using the Compound–Protein Interaction (CPI) task with two datasets: Human and C. elegans. The Human dataset has 3369 positive interactions between 1052 compounds and 852 proteins, while the C. elegans dataset has 4000 interactions between 1434 compounds and 2504 proteins. Positive samples come from DrugBank and matador databases, and negative samples from a virtual screening framework. Model performance is assessed using AUC, Precision, Recall, and F1-score.The calculation formulas are shown in Equation 13 and Equation 14:

$$Precision = \frac{TP}{TP + FP} \tag{13}$$

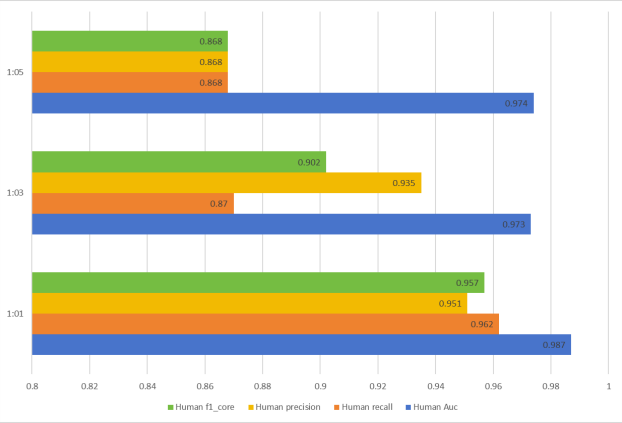

Figure 3. *The performance on human dataset*

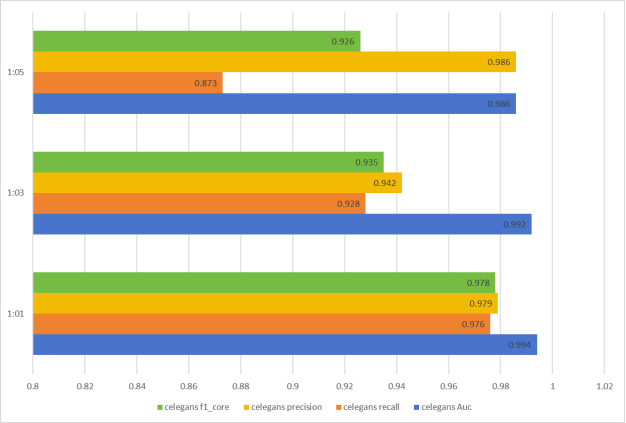

Figure 4. *The performance on C.elegans dataset*

$$Recall = \frac{TP}{TP+FN} \tag{14}$$

Among them, TP represents true positives, that is, the number of samples correctly predicted as positive by the model; FP represents false positives, that is, the number of negative samples incorrectly classified as positive by the model; FN represents false negatives, that is, the situation where positive samples are misclassified as negative by the model. The F1-score is a comprehensive evaluation metric for a model's classification performance, particularly suitable for assessing model performance in cases of data imbalance. It is the harmonic mean of Precision and Recall. The F1-score takes into account both precision and recall, with the calculation formula shown in Equation 15:

$$F1-score = \frac{2*Precision*Recall}{Precision+Recall} \tag{15}$$

The experiment used five-fold cross-validation, where each dataset is randomly divided into five equal-sized parts, with each part used in turn to validate the performance of the model trained on the other four parts. Within WGNN-DTA, they assessed the method's performance when the ratio of positive to negative samples was set to 1:1, 1:3, and 1:5, and we adopted the same setup. The performance of the model on the two datasets is shown in Figure 3 and Figure 4.

The results indicate that the TAW-DTA model exhibits high performance, with AUC metrics exceeding 0.9 in five-fold cross-validation. Optimal model performance is observed at a 1:1 ratio of positive to negative samples. However, with an increasing proportion of negative samples, the model's performance gradually worsens, and the standard deviation rises, which indicates that the model's stability is decreasing. This phenomenon arises from the diminished fitting capacity of the model induced by data imbalance. Even so, TAW-DTA maintains good performance even when the sample ratio reaches 1:5.

Conclusion

This study introduces TAW-DTA, an advanced deep learning framework for drug-target affinity prediction. By addressing the limitations of shallow graph neural networks (GNNs) and static convolution filters, the proposed model leverages TAGCN to adaptively capture topological features of molecular graphs and protein contact maps, while the gated skip-connection mechanism enhances feature preservation across deep layers. Experimental results on Davis and KIBA datasets demonstrate superior performance over existing models, achieving higher CI scores (0.003 and 0.001 improvements, respectively) and robust generalization. Ablation analyses highlight the critical roles of TAGCN in structural feature extraction and skip-connections in mitigating training instability. The framework not only advances DTA prediction accuracy but also provides interpretable insights into molecular interactions, paving the way for efficient drug discovery pipelines.

Acknowledgment

This work was supported by the Shandong Natural Science Foundation under Grants ZR2024MF102, ZR2023MF008, the National Natural Science Foundation of China under Grant 62372468, the Major Basic Research Projects in Shandong Province under Grant ZR2023ZD32, the Qingdao Natural Science Foundation under Grant 23-2-1-161-zyyd-jch, the research and development of key technologies for clinical medicine of "heart brain treatment", Yunnan Province, under Grant No.202203AC100007, the State Key Laboratory of Shale Oil and Gas Enrichment Mechanisms and Effective Development under Grant No.33550000-22-ZC0613-0243, and the Jinan Clinical Medical Science and Technology Innovation Plan under Grant 202225018.

References

[1] Wouters, Olivier J., Martin McKee, and Jeroen Luyten. "Research and development costs of new drugs—reply." Jama 324.5 (2020): 518-518.

[2] Yang, Hongpeng, et al. "Drug–disease associations prediction via multiple kernel-based dual graph regularized least squares." Applied Soft Computing 112 (2021): 107811.

[3] Jiang M, Wang S, Zhang S, Zhou W, Zhang Y, Li Z. Sequence-based drug-target affinity prediction using weighted graph neural networks. BMC Genomics. 2022 Jun 17;23(1):449. doi: 10.1186/s12864-022-08648-9. PMID: 35715739; PMCID: PMC9205061.

[4] Jumper, J.; Evans, R.; Pritzel, A.; Green, T.; Figurnov, M.; Ronneberger, O.; Tunyasuvunakool, K.; Bates, R.; Žídek, A.; Potapenko,

A.; et al. Highly accurate protein structure prediction with AlphaFold. Nature 2021, 596, 583–589.

[5] Rives, A.; Meier, J.; Sercu, T.; Goyal, S.; Lin, Z.; Liu, J.; Guo, D.; Ott, M.; Zitnick, C.L.; Ma, J.; et al. Biological structure and function emerge from scaling unsupervised learning to 250 million protein sequences. Proc. Natl. Acad. Sci. USA 2021, 118, e2016239118.

[6] Baek, M.; DiMaio, F.; Anishchenko, I.; Dauparas, J.; Ovchinnikov, S.; Lee, G.R.; Wang, J.; Cong, Q.; Kinch, L.N.; Schaeffer, R.D.; et al. Accurate prediction of protein structures and interactions using a three-track neural network. Science 2021, 373, 871–876.

[7] Rao R, Meier J, Sercu T, Ovchinnikov S, Rives A. Transformer protein language models are unsupervised structure learners. In: International Conference on Learning Representations: 2020.

[8] Landrum G. RDKit: Open-source cheminformatics. 2006[J]. Google Scholar, 2006.

[9] Davis M I, Hunt J P, Herrgard S, et al. Comprehensive analysis of kinase inhibitor selectivity[J]. Nature biotechnology, 2011, 29(11): 1046-1051.

[10] J. Tang, A. Szwajda, S. Shakyawar, T. Xu, P. Hintsanen, K. Wennerberg, and T. Aittokallio, "Making sense of large-scale kinase inhibitor bioactivity data sets: a comparative and integrative analysis," Journal of Chemical Information and Modeling, vol. 54, no. 3, pp. 735–743, 2014.

[11] S. A. Hollingsworth and R. O. Dror, "Molecular dynamics simulation for all," Neuron, vol. 99, no. 6, pp. 1129–1143, 2018.

[12] Li, H., Leung, K.-S., Wong, M.-H., and Ballester, P. (2015). Low-quality structural and interaction data improves binding affinity prediction via random forest. Molecules 20,10947–10962. doi:10.3390/molecules200610947

[13] Ballester, P. J., and Mitchell, J. B. O. (2010). A machine learning approach to predicting protein–ligand binding affinity with applications to molecular docking.Bioinformatics 26, 1169–1175. doi:10.1093/bioinformatics/btq112

[14] Li Zhang, Chun-Chun Wang, Xing Chen, Predicting drug–target binding affinity through molecule representation block based on multi-head attention and skip connection, Briefings in Bioinformatics, Volume 23, Issue 6, November 2022, bbac468, https://doi.org/10.1093/bib/bbac468

[15] Yuni Zeng, Xiangru Chen, Yujie Luo, Xuedong Li, Dezhong Peng, Deep drug-target binding affinity prediction with multiple attention blocks, Briefings in Bioinformatics, Volume 22, Issue 5, September 2021, bbab117, https://doi.org/10.1093/bib/bbab117

[16] Nguyen T, Le H, Quinn TP, Nguyen T, Le TD, Venkatesh S. GraphDTA: predicting drug-target binding affinity with graph neural networks. Bioinformatics. 2021 May 23;37(8):1140-1147. doi: 10.1093/bioinformatics/btaa921. PMID: 33119053.

[17] Zhang, L., Ouyang, C., Liu, Y., Liao, Y., and Gao, Z. (2023a). Multimodal contrastiverepresentation learning for drug-target binding affinity prediction. Methods 220,126–133. doi:10.1016/j.ymeth.2023.11.005

[18] Mukherjee, Shrimon, Madhusudan Ghosh, and Partha Basuchowdhuri. "DeepGLSTM: deep graph convolutional network and LSTM based approach for predicting drug-target binding affinity." Proceedings of the 2022 SIAM international conference on data mining (SDM). Society for Industrial and Applied Mathematics, 2022.

[19] Yang, Ziduo, et al. "MGraphDTA: deep multiscale graph neural network for explainable drug–target binding affinity prediction." Chemical science 13.3 (2022): 816-833.

[20] Jiang, Mingjian, et al. "Drug–target affinity prediction using graph neural network and contact maps." RSC advances 10.35 (2020): 20701-20712.

[21] Zhu, Z., Yao, Z., Zheng, X., Qi, G., Li, Y., Mazur, N., et al. (2023c). Drug–target affinityprediction method based on multi-scale information interaction and graphoptimization. Comput. Biol. Med. 167, 107621. doi:10.1016/j.compbiomed.2023.107621

[22] Du, Jian, et al. "Topology adaptive graph convolutional networks." arxiv preprint arxiv:1710.10370 (2017).

Author Biography

Linman Du is currently pursuing his master's degree at the School of Control Science and Engineering, China University of Petroleum (Huadong). His research interests include computer vision and medical image processing.

Wenzong Jiang received his Master's degree in Information and Communication Engineering from China University of Petroleum (Huadong). His research interests include computer vision and medical image processing.

Bin Shen is Engineering Director (AI/ML) at Celonis. He was with the Advanced Technology Group (ATG) of Pinterest from 2019 to 2022. Before that, he was with Google New York from 2015 to 2019. Bin earned B.S. and M.S. degrees from Department of Electronic Engineering, Tsinghua University, Beijing, in 2007 and 2009, respectively, and M.S. and Ph.D. degrees from Department of Computer Science, Purdue University, West Lafayette, Indiana, in 2011 and 2014.

Weifeng Liu is a Professor at the College of Control Science and Engineering, China University of Petroleum (East China). He holds a Ph.D. in pattern recognition and intelligent systems from the University of Science and Technology of China. His research interests include pattern recognition and machine learning, and he has published extensively in top journals. He serves as an associate editor for Neural Processing Letters and co-chair for the IEEE SMC technical committee.

Baodi Liu received the Ph.D. degree in electronic engineering from Tsinghua University, Beijing, China. He is currently an Associate Professor with the College of Control Science and Engineering, China University of Petroleum, Qingdao, China. His research interests include computer vision and machine learning.

JOIN US AT THE NEXT EI!

electronic IMAGING

Imaging across applications . . . Where industry and academia meet!

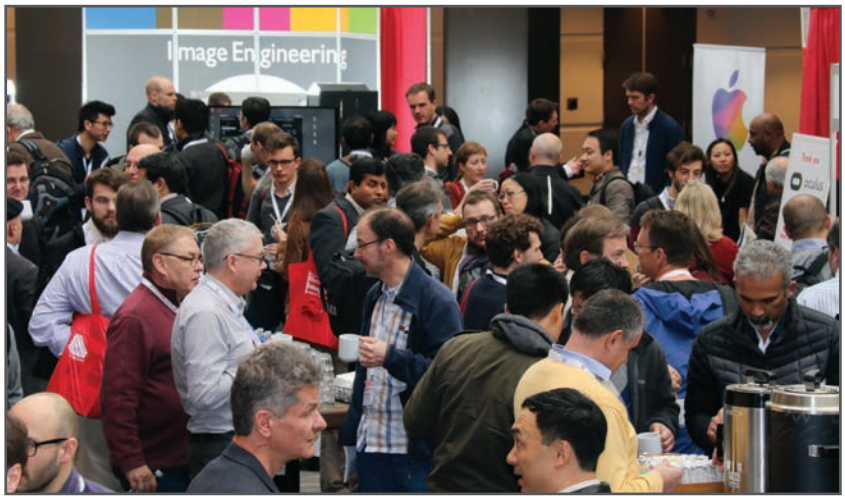

• SHORT COURSES • EXHIBITS • DEMONSTRATION SESSION • PLENARY TALKS •
• INTERACTIVE PAPER SESSION • SPECIAL EVENTS • TECHNICAL SESSIONS •

www.electronicimaging.org

ADVANCING IMAGING SCIENCE 75 1947 IS&T 2022 imaging.org